# Hybridization of Surface Waves with Organic Adlayer Librations: A Helium Atom Scattering and Density Functional Perturbation Theory Study of Methyl-Si(111)

Ryan D. Brown,[1] Zachary M. Hund,[1] Davide Campi,[2] Leslie E. O'Leary,[3] Nathan S. Lewis,[3] M. Bernasconi,[2] G. Benedek,[2,4] and S. J. Sibener[1,*]

[1]*The James Franck Institute and Department of Chemistry, The University of Chicago, 929 East 57th Street, Chicago, Illinois 60637, USA*

[2]*Dipartimento di Scienza dei Materiali, Universita di Milano-Bicocca, Via Cozzi 53, 20125 Milano, Italy*

[3]*Beckman Institute and Kavli Nanoscience Institute, Division of Chemistry and Chemical Engineering, 210 Noyes Laboratory, 127-72, California Institute of Technology, Pasadena, California 91125, USA*

[4]*Donostia International Physics Center (DIPC), Universidad the País Vasco (EHU) 20018 Donostia/San Sebastian, Spain*

(Received 1 February 2013; published 9 April 2013)

The interplay of the librations of a covalently bound organic adlayer with the lattice waves of an underlying semiconductor surface was characterized using helium atom scattering in conjunction with analysis by density functional perturbation theory. The Rayleigh wave dispersion relation of $CH_3$- and $CD_3$-terminated Si(111) surfaces was probed across the entire surface Brillouin zone by the use of inelastic helium atom time-of-flight experiments. The experimentally determined Rayleigh wave dispersion relations were in agreement with those predicted by density functional perturbation theory. The Rayleigh wave for the $CH_3$- and $CD_3$-terminated Si(111) surfaces exhibited a nonsinusoidal line shape, which can be attributed to the hybridization of overlayer librations with the vibrations of the underlying substrate. This combined synthetic, experimental, and theoretical effort clearly demonstrates the impact of hybridization between librations of the overlayer and the substrate lattice waves in determining the overall vibrational band structure of this complex interface.

DOI: 10.1103/PhysRevLett.110.156102 PACS numbers: 68.35.Ja, 63.20.D−, 68.47.Fg, 79.20.Rf

The realization that unsaturated hydrocarbons can form covalent bonds to semiconductor interfaces has spawned a rapid evolution in the tailoring of interfacial properties using bound organic adlayers [1]. Such organic-terminated Si surfaces exhibit improved oxidative and electrochemical stability relative to hydrogen-terminated silicon for applications including, for example, photoelectrodes in electrochemical cells [2–4], and biosensing electronics [5,6]. Precise knowledge of bonding and dynamical properties of such decorated interfaces can be acquired by combining experimental measurements of the surface wave dispersions across the entire surface Brillouin zone (SBZ) with complementary electronic structure calculations [7–9]. To date, such studies have focused on chemically functionalized metal surfaces [10–12]. We describe the extension of these experimental and theoretical techniques to elucidate the surface vibrations of organic-semiconductor hybrid interfaces.

Silicon surfaces have been functionalized using alkyl termination *via* radical intermediates [13,14], the Diels-Alder addition of dienes [15], and the Grignard addition of alkyl terminal groups [16], as well as other methods. Methyl termination has emerged as an alternative to hydrogen termination for Si(111) interfaces due to the passivation of surface reconstruction and the demonstrably superior resistance to oxidation of $CH_3$-Si(111) relative to H-Si(111) [14,16]. The impact of the C-Si bond on the surface electronic band structure [17], on the surface termination and structure [18], and on the vibrations of the terminal methyl groups [19–21] has been elucidated, but the effect that methyl termination has on the vibrational band structure of the underlying silicon lattice remains unexplored. Helium atom scattering (HAS) has been used to characterize vibrations in low density alkanethiols on gold [22], as well as to probe the thermal motion and extent of structural perfection of both $CH_3$-Si(111)-$(1 \times 1)$ and $CD_3$-Si(111)-$(1 \times 1)$ [23]. We describe herein a notable extension to the understanding of organically terminated semiconductor interfaces through a successful interrogation of the surface phonon dispersion relations.

In this Letter we present the first characterization of the surface phonon dispersion relations across the entire SBZ for $CH_3$ and $CD_3$-Si(111) *via* angle- and energy-resolved inelastic single-phonon scattering measurements. The experimental data have been leveraged by complementary, quantitative density functional perturbation theory (DFPT) calculations. This combined approach allows for the examination of the interplay of the interatomic force constants, mass loading, and adlayer vibrations in determining the surface vibrations of this interface. These results have been compared to the surface dispersion relations of a simpler adsorbate system, H-Si(111)-$(1 \times 1)$ [24,25], to study the interaction of the overlayer vibrations with those of the underlying substrate. H-Si(111) provides a suitable candidate for comparison because the H-Si(111) interface exhibits surface dynamics that are similar to those of the unreconstructed Si(111) interface [26], and thus the

 

overlayer interactions do not significantly perturb the vibrational characteristics of the semiconductor lattice.

Methyl-terminated Si(111) wafers were prepared by a two-step chlorination-alkylation process, and shipped from the California Institute of Technology to the University of Chicago under argon. Upon arrival, the samples were sonicated in 1:1 methanol:water, and then were mounted in the scattering chamber of an ultrahigh vacuum (UHV) helium atom scattering apparatus [27]. The supersonic helium beam ($E_B = 38$–$65$ meV, $\Delta v/v \leq 1\%$) was produced in a differentially pumped chamber, and was modulated by mechanical chopping. A series of apertures collimated the beam to a 4 mm spot size on a target (chopper-to-crystal distance of 0.4996 m) that was mounted onto a six-axis manipulator in a UHV scattering chamber (base pressure $3 \times 10^{-10}$ torr). Postcollision He atoms were scattered into a rotatable detector arm (crystal-to-ionizer distance of 0.5782 m) with an angular resolution of 0.45° FWHM, and the atoms were detected through electron bombardment ionization followed by quadrupole mass selection. The experimental dispersion curves were obtained from time-of-flight (TOF) spectra. The precision of the measurement was conservatively estimated by the energy distribution of a room temperature beam to be $\pm 0.5$ meV, with improved precision at lower beam energies. The precision of the momentum transfer varied with position and beam energy, but typically was on the order of $10^{-2}$ Å$^{-1}$.

The dynamical properties of the $CH_3$-Si(111) and $CD_3$-Si(111) surfaces were calculated using DFPT, as implemented in the QUANTUM-ESPRESSO package [28], using Ultrasofts pseudopotentials and the Perdew-Burke-Ernzerhof (PBE) [29] approximation for the exchange-correlation energy functional. The electronic wave functions were expanded in plane waves up to a 28 Ry energy cutoff and a 280 Ry charge density cutoff. The modeled surface consisted of a slab geometry that contained 12 silicon atom layers with methyl groups adsorbed on both sides, with the slabs separated by a 12 Å vacuum gap. The SBZ was sampled over a Monkhorst-Pack grid of $6 \times 6 \times 1$ [30]. The atomic positions were relaxed until the forces were below a 0.1 mRy/au threshold. The slab thickness was increased to 30 layers through the insertion of bulk layers with *ab initio* bulk force constants between relaxed surface layers. The surface force constants were obtained by interpolation of a $6 \times 6 \times 1$ $q$-point mesh for the SBZ, while the bulk force constants were obtained from a similar calculation employing a $6 \times 6 \times 3$ $q$-point mesh.

For in-plane helium atom scattering, the kinematic conditions, conservation of energy [Eq. (1)], and conservation of crystal momentum [Eq. (2)], collectively constrain the observable energy and parallel momentum exchanges through the functional form of a scan curve [Eq. (3)].

$$E_f = E_i \pm \hbar\omega(Q), \tag{1}$$

$$\Delta K = k_f \sin\theta_f - k_i \sin\theta_i = Q + G_{mn}, \tag{2}$$

$$\Delta E = E_i\left[\frac{(\sin\theta_i + \Delta K/k_i)^2}{\sin^2\theta_f} - 1\right]. \tag{3}$$

In the equations above, $E_i$ and $E_f$ are the incident and scattered translational energies, respectively, $\theta_i$ and $\theta_f$ are the respective incident and scattered angles from the surface normal, $K$ is the parallel (in plane) component of the helium atom wave vector, $k_i$ is the incident wave vector, $Q$ is the phonon wave vector, and $G_{mn}$ is a reciprocal lattice vector. Time-of-flight spectra were obtained at a variety of kinematic conditions and beam energies (38–65 meV) for both the $\langle 01\bar{1}\rangle$, $\overline{\Gamma M}$, and $\langle 11\bar{2}\rangle$, $\overline{\Gamma K}$, crystallographic directions, Fig. 1(a). TOF spectra obtained at the same beam energy and angle of incidence with different scattering angles are shown in Fig. 1(c). Only data for which the phonon excitations were sufficiently resolved from that of the bulk band edge, and which showed clear dispersion under several scattering conditions, were attributed to the Rayleigh wave (RW). These spectra clearly show the dispersion of the RW near the zone center for the $\overline{\Gamma K}$ direction. Many such measurements allowed the complete mapping of the RW dispersion across the SBZ. Isotopic substitution of $CH_3$ with $CD_3$ allowed for the determination of the contributions from the mass loading effect to changes in the dispersion relations relative to H-Si(111). The mode energy scales as $C^{1/2}M_{\text{eff}}^{-1/2}$, with $C$ being the interatomic force constant and $M_{\text{eff}}$ the effective mass, so this substitution could significantly shift any surface vibrational modes with an effective mass close to that of a methyl group.

The RW dispersion relations obtained from DFPT were in excellent agreement with the HAS measurements for both $CH_3$-Si(111), Fig. 2(a), and $CD_3$-Si(111), Fig. 2(b). For $CH_3$- and $CD_3$-Si(111), inelastic scattering events were observed below the RW along $\overline{\Gamma K}$; these data arise from multiple phonon scattering events. Such multiple phonon inelastic scattering events were only observed in spectra that were obtained with high beam energies of 54 to 63 meV, and are not observed at lower collisional energies. In this beam energy range, and at the sample temperatures used, the Weare parameter is near the threshold of where single phonon scattering dominates [31], thus being consistent with the observation of multiple phonon inelastic collisions. The sagittal polarization of the total atomic displacement of the methyl group, Fig. 2, indicates the shear vertical displacement associated with each mode across the SBZ. HAS is most sensitive to sagittal displacements; thus, the total sagittal displacement is a good guideline for determining the observable modes using neutral atom scattering. The data agree well with the theoretical mode polarization in that single phonon inelastic transitions were observed only where the atomic displacements contain some sagittal component.

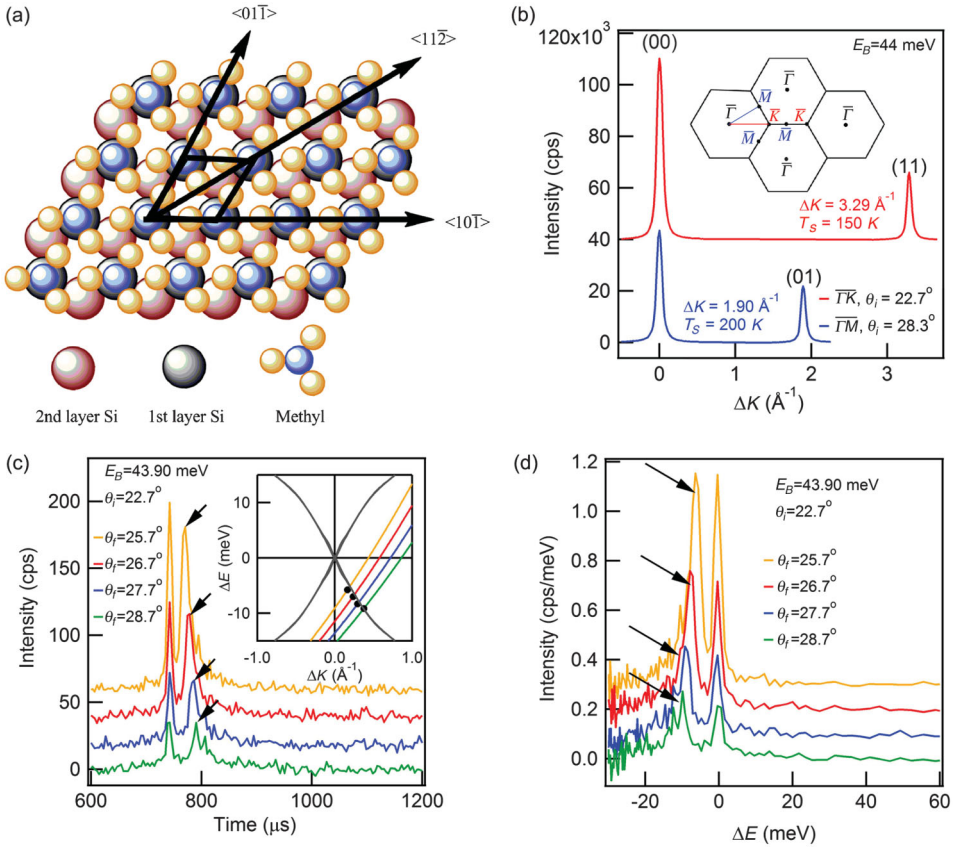


FIG. 1 (color). A schematic of the methyl-terminated Si(111) surface, with the real space unit cell highlighted, showing the crystallographic orientations of the reciprocal lattice $\overline{\Gamma M}$, $\langle 01\bar{1}\rangle$, and $\overline{\Gamma K}$, $\langle 11\bar{2}\rangle$ (a). Diffraction spectra for both of these orientations are overlaid along with an inset displaying the reciprocal space unit cell (b). An overlay of TOF spectra from the $CH_3$-Si(111) surface at $T_S = 150$ K along $\overline{\Gamma K}$ (c). The arrows indicate single-phonon creation peaks, and the inset displays scan curves for each spectrum (colors). The black points indicate the energy and momentum transfers for the observed inelastic peaks, and the gray lines are the Rayleigh wave dispersion curves. (d) is the corresponding energy transfer spectra of the TOF data from (c), with inelastic peaks indicated by black arrows. Spectra are offset for clarity.

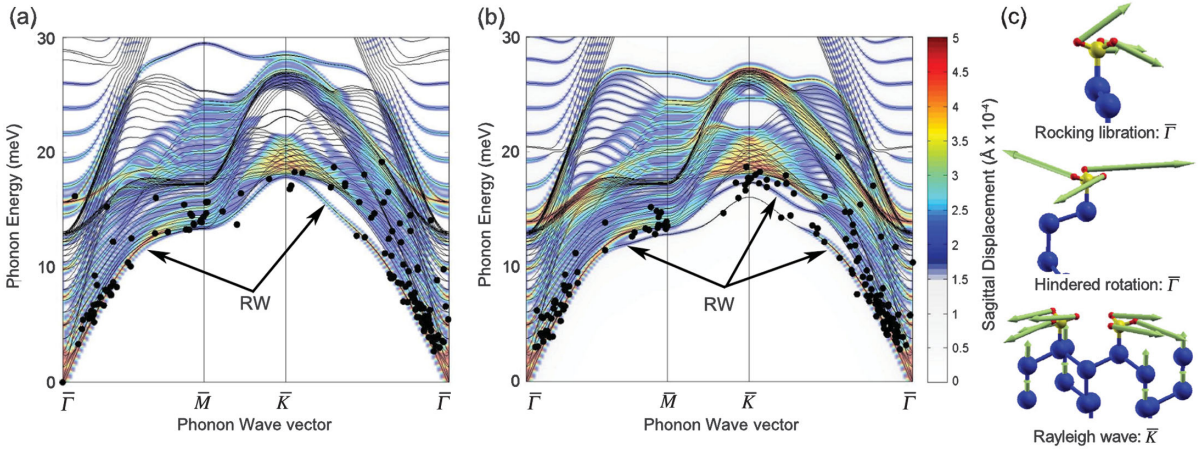


FIG. 2 (color). HAS single phonon data overlaid on the dispersion curves (black lines) obtained from DFPT calculations for (a) $CH_3$-Si(111) and (b) $CD_3$-Si(111). Multiple phonon scattering events are not shown here for improved clarity. The total sagittal displacement of the terminal $CH_3$ and $CD_3$ groups is presented in the color scale. The single phonon HAS data coincide with modes that contain significant sagittal displacements. Schematics of the displacement patterns for the rocking libration, the hindered rotation, and the RW are presented, with arrows proportional to the real components of the mode eigenvectors (c).

At the $\bar{M}$ point, the RW energies for both the $CH_3$ and $CD_3$ terminated surfaces are almost resonant with the bulk transverse acoustic band, and the proximity to the energy of the band edge is within the precision of the helium atom scattering measurements. The energies of the RW, as obtained from theory, are 13.3 and 17.9 meV for the $\bar{M}$ and $\bar{K}$ points, respectively, on the $CH_3$-Si(111) surface, and are 13.4 and 17.3 meV for the $\bar{M}$ point and $\bar{K}$ points, respectively, on the $CD_3$-Si(111) surface. On the $CD_3$-Si(111) surface, the RW crosses with the hindered rotation of the $CD_3$ group about the C-Si bond axis, and thus the lowest band (about 16 meV) at $\bar{K}$ is this surface libration. The RW frequency is very similar for $CH_3$-Si(111), $CD_3$-Si(111), and H-Si(111) [25] at the $\bar{M}$ point but deviates significantly along the $\overline{\Gamma K}$ azimuth. For the two alkyl terminated surfaces, the $\bar{K}$ point frequency is higher than that of H-Si (111) and the RW dispersion relation deviates from a normal sinusoidal shape as it evolves across the SBZ.

The H-Si(111) and $CH_3$-Si(111) surfaces showed quantitatively similar surface charge distributions, based on a comparison of the silicon lattice charge density for both interfaces. The methyl-terminated surface exhibited a small ($7.0\times10^{-4}$ atomic unit) charge density increase in the region above the second layer Si atom as compared to the H-terminated surface, while $CH_3$-Si(111) exhibited a $2.1\times10^{-4}$ atomic unit reduction of charge density between the second and third layer Si atoms relative to H-termination. These minor variations in the $CH_3$-Si(111) surface charge density of the silicon lattice resulted in a decrease in the calculated Si-Si force constants in the first silicon bilayer of about 6% with respect to H-Si(111). The lack of significant differences in the silicon lattice charge densities of these two surfaces indicates that altered local force constants are not solely responsible for the deviation in the methyl-Si(111) RW dispersion relative to H-Si(111). Rather, changes to the RW dispersion relation, as shown below, can be attributed to interactions with adlayer librations.

The displacement fields that were obtained from the DFPT calculations did not exhibit the linear sagittal polarization at the $\bar{M}$ point that is expected for the Rayleigh wave of an ideal fcc surface [7]. Instead, the surface waves of the Si lattice hybridized with a low energy libration of the methyl group. The two librational modes of particular interest for the $CH_3$-Si(111) and $CD_3$-Si(111) interfaces are a hindered rotation about the Si-C axis and a rocking libration that involves a bending of the Si-C bond angle, Fig. 2(c). The hybridization occurs between the rocking libration and the Rayleigh wave, Fig. 2(c). Unlike H-Si (111), in which the motion of the hydrogen is adiabatic with respect to the underlying lattice [32], the rocking libration of the methyl group couples with the underlying lattice wave near the zone edges, inducing an observable deviation of the Rayleigh wave dispersion along $\overline{\Gamma K}$ [33]. To confirm the role of methyl librations in perturbing the RW energy and lineshape relative to the properties of H-Si(111), DFPT calculations were employed that simulated a "frozen" surface methyl group. The methyl group was removed, with the surface silicon atom's mass artificially modified to be the sum of a silicon atom and a methyl group, and the dispersion curves were obtained using the silicon force field obtained in the earlier calculations. The actual $CH_3$-Si(111) and $CD_3$-Si(111) curves deviate from the frozen calculation curves near the same region of the SBZ, Fig. 3, although the exact location of the crossing of modes in the $CD_3$ terminated surface was difficult to discern. The curves obtained from the frozen calculations were in excellent accord with those of H-Si (111), with only a minor decrease in frequency due to mass loading between the two methyl isotopes. At the $\bar{K}$ point, the frozen $CD_3$-Si(111) curves exhibited a RW energy that was depressed by less than 1 meV with respect to $CH_3$-Si(111), which is to the same degree as the depression observed in the actual curves, so the treatment of mass loading is appropriate.

These results indicate that the mass loading effect and changes to the local force field induced by the C-Si dipole are not responsible for deviations in the RW energy and line shape for the methyl-terminated surfaces with respect to H-Si(111). Rather, the hybridization of the lattice waves with the organic adlayer rocking libration is responsible for the increased energy at the $\bar{K}$ point and for the nonsinusoidal dispersion relation of the RW. This behavior is in

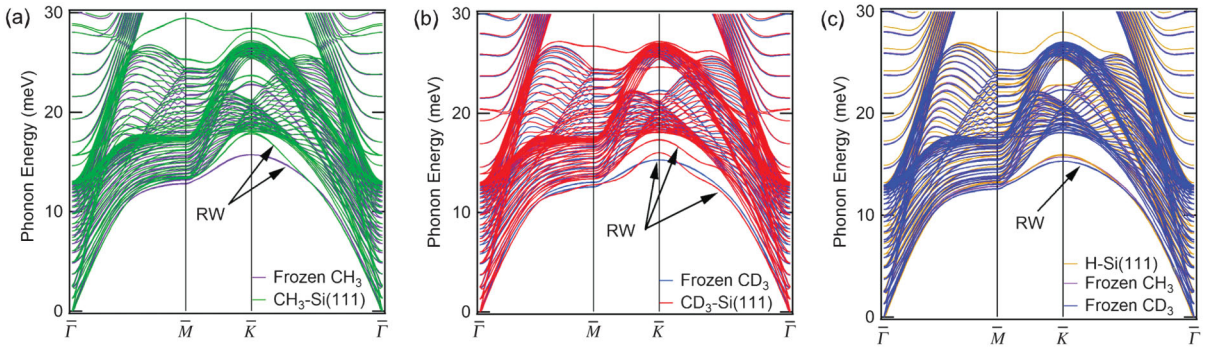


FIG. 3 (color). Overlay of the actual curves with the "frozen" calculations for $CH_3$-, (a), and $CD_3$-Si(111), (b). (c) overlays the frozen curves with those obtained from H-Si(111) calculations.

contrast to similar experiments and calculations performed for As : Si(111)-(1 × 1), in which the heavier mass substitution of arsenic was the primary contributor to changes in the surface wave energies [26].

These HAS and DFPT studies of alkyl-terminated Si (111) have demonstrated the importance of adlayer librations in determining the overall vibrational band structure of surface waves, and show the power of combining these techniques for examining the vibrational characteristics of a hybrid organic-semiconductor interface. In the case of silicon, alkyl termination has been a successful strategy for tailoring interfacial properties. We have shown that the consequence of such functionalization is the perturbation of the interfacial phonons due to coupling between adlayer and lattice vibrations. These results have revealed new aspects of interfacial vibrational dynamics for organic-functionalized semiconductor interfaces.

S. J. S. would like to acknowledge the support of the Air Force Office of Scientific Research Grant No. FA9550-10-1-0219, and the Material Research Science and Engineering Center at the University of Chicago for infrastructure support. N. S. L. acknowledges support from NSF-CHE1214152, and L. E. O. was funded by a Link foundation Energy fellowship.

*Corresponding author.
s-sibener@uchicago.edu

[1] H. N. Waltenburg and J. T. Yates, Chem. Rev. **95**, 1589 (1995).
[2] A. Bansal and N. S. Lewis, J. Phys. Chem. B **102**, 4058 (1998).
[3] T. Osaka, M. Matsunaga, S. Kudo, D. Niwa, Y. Shacham-Diamand, W. Jaegermann, and R. Hunger, J. Electrochem. Soc. **154**, H919 (2007).
[4] X. Shen, B. Sun, F. Yan, J. Zhao, F. Zhang, S. Wang, X. Zhu, and S. Lee, ACS Nano **4**, 5869 (2010).
[5] T. L. Lasseter, B. H. Clare, N. L. Abbott, and R. J. Hamers, J. Am. Chem. Soc. **126**, 10 220 (2004).
[6] W. Yang and R. J. Hamers, Appl. Phys. Lett. **85**, 3626 (2004).
[7] G. Benedek and J. P. Toennies, Surf. Sci. **299–300**, 587 (1994).
[8] D. Farias and K. H. Rieder, Rep. Prog. Phys. **61**, 1575 (1998).
[9] G. Benedek, M. Bernasconi, V. Chis, E. Chulkov, P. M. Echenique, B. Hellsing, and J. P. Toennies, J. Phys. Condens. Matter **22**, 084020 (2010).
[10] T. S. Rahman, D. L. Mills, J. E. Black, J. M. Szeftel, S. Lehwald, and H. Ibach, Phys. Rev. B **30**, 589 (1984).
[11] K. D. Gibson and S. J. Sibener, Phys. Rev. Lett. **55**, 1514 (1985).
[12] K. Kern, R. David, R. L. Palmer, G. Comsa, J. He, and T. S. Rahman, Phys. Rev. Lett. **56**, 2064 (1986).
[13] M. R. Linford and C. E. D. Chidsey, J. Am. Chem. Soc. **115**, 12 631 (1993).
[14] M. R. Linford, P. Fenter, P. M. Eisenberger, and C. E. D. Chidsey, J. Am. Chem. Soc. **117**, 3145 (1995).
[15] A. V. Teplyakov, M. J. Kong, and S. F. Bent, J. Am. Chem. Soc. **119**, 11 100 (1997).
[16] A. Bansal, X. Li, I. Lauermann, N. S. Lewis, S. I. Yi, and W. H. Weinberg, J. Am. Chem. Soc. **118**, 7225 (1996).
[17] R. Hunger, R. Fritsche, B. Jaeckel, W. Jaegermann, L. J. Webb, and N. S. Lewis, Phys. Rev. B **72**, 045317 (2005).
[18] H. Yu, L. J. Webb, R. S. Ries, S. D. Solares, W. A. Goddard, J. R. Heath, and N. S. Lewis, J. Phys. Chem. B **109**, 671 (2005).
[19] L. J. Webb, S. Rivillon, D. J. Michalak, Y. J. Chabal, and N. S. Lewis, J. Phys. Chem. B **110**, 7349 (2006).
[20] T. Yamada, M. Kawai, A. Wawro, S. Suto, and A. Kasuya, J. Chem. Phys. **121**, 10 660 (2004).
[21] G. A. Ferguson and K. Raghavachari, J. Chem. Phys. **125**, 154708 (2006).
[22] A. W. Rosenbaum, M. A. Freedman, S. B. Darling, I. Popova, and S. J. Sibener, J. Chem. Phys. **120**, 3880 (2004).
[23] J. S. Becker, R. D. Brown, E. Johansson, N. S. Lewis, and S. J. Sibener, J. Chem. Phys. **133**, 104705 (2010).
[24] C. Stuhlmann, G. Bogdanyi, and H. Ibach, Phys. Rev. B **45**, 6786 (1992).
[25] R. B. Doak, Y. J. Chabal, G. S. Higashi, and P. Dumas, J. Electron Spectrosc. Relat. Phenom. **54–55**, 291 (1990).
[26] P. Santini, P. Ruggerone, L. Miglio, and R. B. Doak, Phys. Rev. B **46**, 9865 (1992).
[27] B. Gans, P. A. Knipp, D. D. Koleske, and S. J. Sibener, Surf. Sci. **264**, 81 (1992).
[28] P. Giannozzi *et al.*, J. Phys. Condens. Matter **21**, 395502 (2009).
[29] J. P. Perdew, K. Burke, and M. Ernzerhof, Phys. Rev. Lett. **77**, 3865 (1996).
[30] H. J. Monkhorst and J. D. Pack, Phys. Rev. B **13**, 5188 (1976).
[31] J. Weare, J. Chem. Phys. **61**, 2900 (1974).
[32] U. Harten, J. P. Toennies, Ch. Wöll, L. Miglio, P. Ruggerone, L. Colombo, and G. Benedek, Phys. Rev. B **38**, 3305 (1988).
[33] See Supplemental Material at http://link.aps.org/supplemental/10.1103/PhysRevLett.110.156102 for additional details concerning the in-plane polarization characteristics of the interfacial adsorbate-semiconductor phonons.